

700987

#12

Report 997



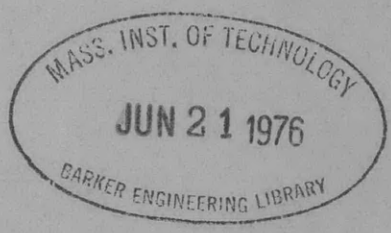
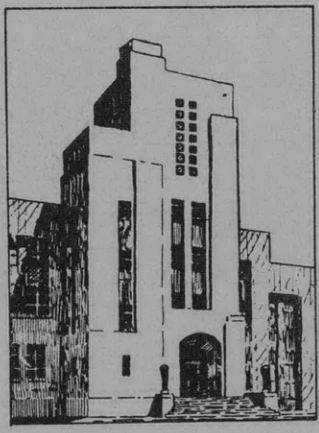
V393  
R46

**NAVY DEPARTMENT**  
**THE DAVID W. TAYLOR MODEL BASIN**  
WASHINGTON 7, D.C.

**AN EXPERIMENTAL INVESTIGATION OF THE SHELL-INSTABILITY  
STRENGTH OF A MACHINED, RING-STIFFENED CYLINDRICAL  
SHELL UNDER HYDROSTATIC PRESSURE  
(MODEL BR-4A)**

by

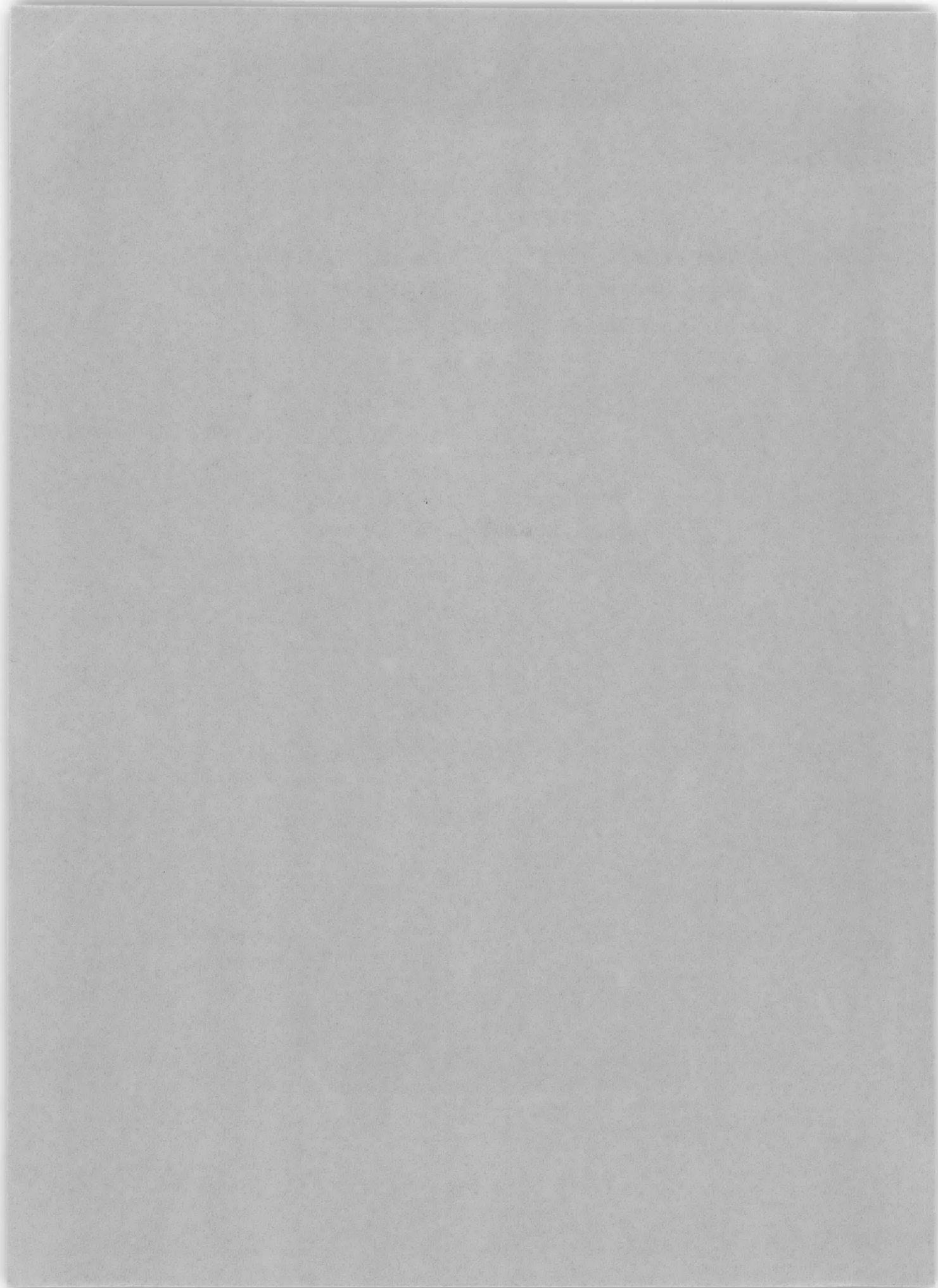
**Arthur F. Kirstein and Robert C. Slankard**



**RESEARCH AND DEVELOPMENT REPORT**

**April 1956**

**Report 997**



**AN EXPERIMENTAL INVESTIGATION OF THE SHELL-INSTABILITY  
STRENGTH OF A MACHINED, RING-STIFFENED CYLINDRICAL  
SHELL UNDER HYDROSTATIC PRESSURE  
(MODEL BR-4A)**

by

**Arthur F. Kirstein and Robert C. Slankard**

**April 1956**

**Report 997  
NS 731-038**

**TABLE OF CONTENTS**

|   | <b>Page</b> |
|---|-------------|
| <b>ABSTRACT</b> .....                           | 1           |
| <b>INTRODUCTION</b> .....                       | 1           |
| <b>DESCRIPTION OF MODEL</b> .....               | 2           |
| <b>TEST APPARATUS AND INSTRUMENTATION</b> ..... | 4           |
| <b>TEST PROCEDURE AND RESULTS</b> .....         | 5           |
| <b>DISCUSSION OF RESULTS</b> .....              | 11          |
| <b>Deflections</b> .....                        | 11          |
| <b>Strains</b> .....                            | 14          |
| <b>Collapse Pressure</b> .....                  | 17          |
| <b>Model Comparison</b> .....                   | 17          |
| <b>CONCLUSIONS</b> .....                        | 19          |
| <b>RECOMMENDATIONS</b> .....                    | 19          |
| <b>ACKNOWLEDGMENT</b> .....                     | 19          |
| <b>REFERENCES</b> .....                         | 20          |

## LIST OF ILLUSTRATIONS

|   | Page |
|---|------|
| Figure 1 - Schematic Drawing of Models.....   | 3    |
| Figure 2 - Apparatus Used for Test of Model BR-4A .....   | 5    |
| Figure 3 - Circularity Plot Showing Radial Displacements at Bay Midway<br>Between Rings (Station 6) ..... | 7    |
| Figure 4 - Internal View of Model BR-4A After Failure .....   | 8    |
| Figure 5 - External View of Model BR-4A After Failure .....   | 8    |
| Figure 6 - Exterior View of Final Collapse Pattern of Models BR-4 and BR-4A .....                         | 9    |
| Figure 7 - Linear Variation of Strain with Pressure at Successive Pressure<br>Loadings.....               | 11   |
| Figure 8 - Strain Sensitivities at Outer Surface of Station 4 at Midbay .....                             | 12   |
| Figure 9 - Circumferential Strain Sensitivities on the Outer Surface of<br>Ring at Station 5 .....        | 13   |
| Figure 10 - Variation of Stress at Interior of Shell with Pressure .....                                  | 15   |
| Figure 11 - Theoretical and Experimental Distribution of Circumferential Strain<br>Sensitivity.....       | 15   |
| Figure 12 - Theoretical and Experimental Distribution of Longitudinal Strain<br>Sensitivity.....          | 16   |

## LIST OF TABLES

|   |    |
|---|----|
| Table 1 - Ratios of Eccentricity to Shell Thickness for Stations Directly Under<br>Rings and Midway Between Rings for Model BR-4A ..... | 6  |
| Table 2 - Pressure Increments for Test of Model BR-4A .....   | 8  |
| Table 3 - Comparison of Theoretical and Experimental Radial Displacement<br>for Model BR-4A .....                                       | 14 |
| Table 4 - Collapse Pressures for Model BR-4A According to Various Theories<br>of Shell Instability .....                                | 17 |
| Table 5 - Comparison of Theoretical and Experimental Radial Displacements for<br>Machined Model BR-4A and Welded Model BR-4.....        | 18 |



## ABSTRACT

The effects of initial eccentricity and residual welding and rolling stresses on the buckling strength of a stiffened cylinder were investigated by tests of a machined and stress-relieved model, Model BR-4A, identical in size and material with a previously tested fabricated model, Model BR-4. The experimental collapse pressure of 550 psi for Model BR-4A agrees well with collapse pressures predicted by theory and, when compared with the collapse pressure of 390 psi for Model BR-4, indicates that initial eccentricity and residual stresses have a decided effect on the strength under external hydrostatic pressure.

## INTRODUCTION

For several years it has been recognized that the most efficient submarine pressure hull is obtained by designing the structure to eliminate the possibility of instability failure. Recent developments suggest, however, that future designs may reintroduce the propensity to a buckling mode of collapse. With the increase in diameter of the pressure hulls to accommodate nuclear power and the ALBACORE hull form, correspondingly thicker material for the shell plating would ordinarily be required. Apart from adding excessive weight, thicker shells would entail fabrication difficulties. To eliminate these problems consideration is being given to thinner plating material of higher yield strength. The geometries associated with such thin plating are likely to introduce a shell-instability type of failure.

Unfortunately, the design equations for predicting shell-instability strength are somewhat unsatisfactory because of the prevailing discrepancy between the experimental and theoretical buckling pressures. These discrepancies are shown in the work of Windenberg<sup>1</sup> and in the more recent tests of Models BR-1, BR-4, and BR-5 at the Taylor Model Basin.<sup>2,3,4</sup> Most investigators have attributed this disparity to the weakening effects of initial out-of-roundness in the shell and stiffening rings and of residual welding or rolling stresses. Even though these effects are known to be present in welded structures, theoretical investigators have been unable to extend their analyses of elastic instability satisfactorily to an imperfect structure with residual stresses. Also, experimenters have been unable to determine quantitatively the deleterious effects of imperfections and residual stresses on the strength of reinforced cylindrical shells. In other words, investigators have been trying to check an elastic theory for a perfect and stress-free structure by testing imperfect welded models. It has now become apparent that the best approach to this problem is first to verify the theory for the perfect structure and then to develop a method for predicting the strength of an imperfect structure.

In this report, results are given from the first of a series of model tests intended to verify the theory for elastic shell instability by testing both machined and stress-relieved cylindrical shells under hydrostatic pressure. This approach to the solution of the *shell-instability* problem was suggested by results obtained from recent tests performed at the

---

<sup>1</sup>References are listed on page 20.

Taylor Model Basin on two groups of machined cylinders<sup>5,6</sup> designed to fail by *general instability*. In this latter case, perfect and imperfect structures are being studied separately, and collapse pressures for models that were stress-relieved and machined agreed well with those predicted by elastic instability theories. Thus it appeared that the discrepancy already noted between theory and experiment for the problem of shell instability must be due to imperfections in the structure.

To test this hypothesis a machined and stress-free model was manufactured which was a geometric duplicate of Model BR-4, a model which had been fabricated by rolling and welding the components in the usual manner. Thus by a comparison of the collapse pressures of these two models, the importance of imperfections could be established.

The machined model, designated BR-4A, its instrumentation, and the testing technique used are described in this report. The experimental results are analyzed and compared with theory. The results from this test are also compared with those obtained during the test of the fabricated Model BR-4. The machined, stress-free Model BR-4A was 29 percent stronger than Model BR-4.

## DESCRIPTION OF MODEL

Model BR-4A was a machined and stress-relieved duplicate of Model BR-4 which was fabricated of separate elements welded together. As shown in Figure 1, both models were ring-stiffened cylindrical shells with four equal bays. The dimensions of the models were:

$$\begin{array}{lll} 2R = 26.820 \text{ in.} & b' = 0.230 \text{ in.} & L = 6.71 \text{ in.} \\ h = 0.132 \text{ in.} & d = 0.95 \text{ in.} & L_f = 7.11 \text{ in.} \end{array}$$

Here  $2R$  is the diameter of the median surface of the shell,  $h$  is the thickness of the shell,  $b'$  and  $d$  are the width and depth of the reinforcing ring, respectively,  $L_f$  is the center-to-center distance between adjacent rings, and  $L$  is the unsupported length between rings. Model BR-4A had 45-deg fillets at the base of the rings, of the same size as the welds on the fabricated model. By duplicating the weld dimensions, it was possible to reproduce the unsupported length between rings and still retain the assumption that two-thirds of the weld acts as a portion of the ring.

The machined model was manufactured at the Norfolk Naval Shipyard. The specifications required a yield strength of material of 50,000 psi ( $\pm 5000$  psi). Specimens taken from the rolled and stress-relieved cylinder (prior to machining) had an average yield strength of 50,600 psi. This value not only coincided with the measured yield strength of BR-4, but the shapes of the stress-strain curves were similar in that they exhibited a definite yield point. By duplicating the yield strengths as well as the geometric proportions, both models had an identical thinness factor  $\lambda$  of 1.103. The only remaining uncontrolled variable was the imperfections in the models due to the two different procedures of fabrication.

A schematic diagram of Model BR-4A is shown in Figure 1b. The model was machined from a rolled cylinder with an inside diameter of 26.25 in. and a wall thickness of 1.50 in. The

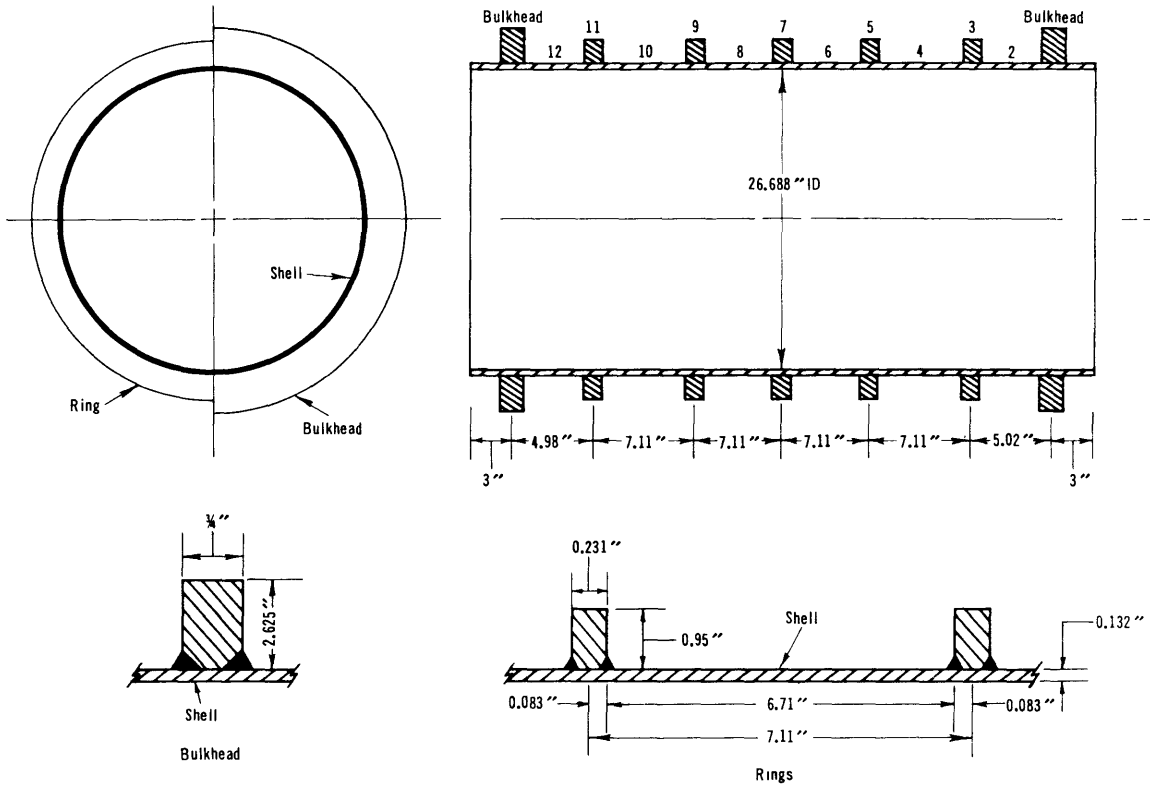


Figure 1a - Fabricated Model BR-4

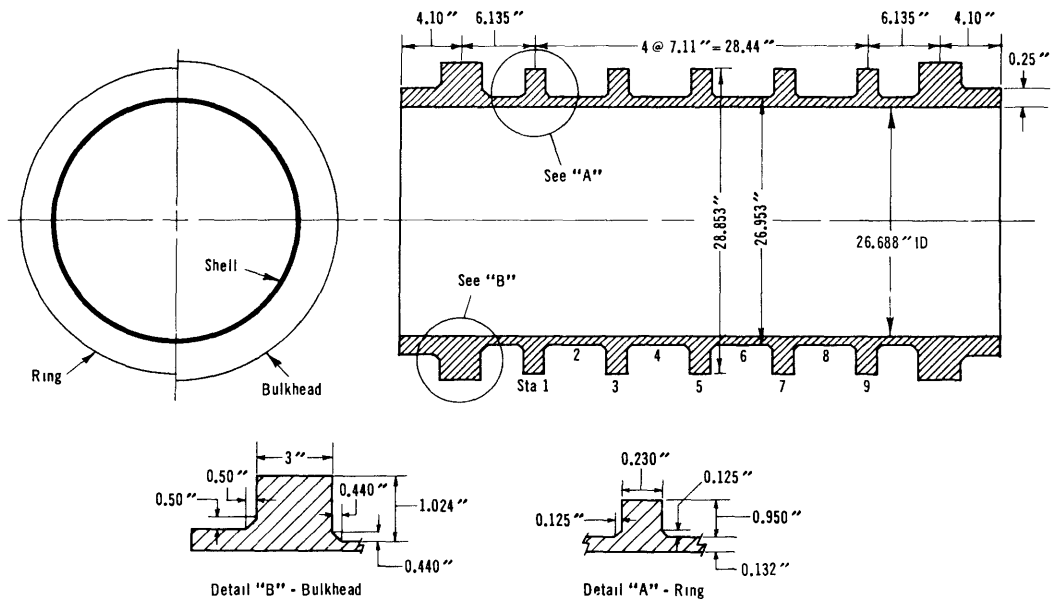


Figure 1b - Machined Model BR-4A

Figure 1 - Schematic Drawing of Models

cylinder was rolled from a flat plate of Grade HT steel and had one longitudinal welded seam. Prior to machining, the formed cylinder was stress-relieved at 1100 deg F for 1 hr. When the model had been rough machined to a wall thickness of 0.5 in., it was again stress-relieved at 1100 deg F for 1 hr. The first stress-relieving process was used to relieve the residual rolling and welding stresses, whereas the second treatment was used to minimize any residual stresses due to distortions in the machining operations.

## TEST APPARATUS AND INSTRUMENTATION

Model BR-4A was tested in the 37-in. diameter hydrostatic-pressure chamber. This pressure chamber has a capacity of 1500 psi. Oil was used as the pressure medium to obviate the necessity of waterproofing the external electrical wire-resistance strain gages.

The external hydrostatic pressure applied to the model was measured with an elastic-tube pressure gage. The gage could be read to the nearest 5 psi throughout the pressure range of the test. As an added check, the pressure was also measured with a Bourdon gage.

Circularity measurements were plotted by the automatic recording deflectometer at eight of the nine stations along the shell. These contours were recorded at 0, 100, 200, 300, 350, 370, 400, and 440 psi. After the displacements at 440 psi had been recorded, the deflectometer was removed so that it would not be damaged should the model suddenly fail. The measurements taken during the test were used to determine the initial eccentricity and to study more closely the displacement of both the rings and the shell under pressure.

Electrical strain gages were installed as follows: The second typical bay, between Stations 3 and 5, was instrumented with pairs of circumferential and longitudinal gages placed along a longitudinal line on the inner and outer surfaces of the shell plating. Nine gage locations were equally spaced along this longitudinal line, which was arbitrarily selected as the zero-deg position on the model. These gages were used to obtain the strain distribution on the shell along a generator to check the elastic theories of Salerno and Pulos<sup>7</sup> and of von Sanden and Gunther.<sup>8</sup>

Longitudinal and circumferential strain gages were also distributed on the outer surface of the shell at Station 4, midway between the rings. These gages were intended to indicate the degree of uniformity of the strains around the shell and to pick up any embryonic lobe formation that might occur. Since a 10-lobe buckling configuration was expected, the gages were spaced at 8-deg arc lengths center-to-center, in order to insure adequate instrumentation to pick up possible lobe formations.

The reinforcing ring at Station 5 was also instrumented with a belt of strain gages. These gages were circumferentially oriented on the outer fibers of the ring and were spaced at 12-deg arc lengths center-to-center. This instrumentation was also intended to indicate the degree of uniformity of strains in the model.

In addition to the specific reasons for each group or belt of strain gages, a more general aim was intended. The  $\lambda$  value for this model was 1.103, which is in the transition range where

either a yield or a shell-instability (buckle) mode of failure could occur. Thus the strain gages on the shell served the important purpose of indicating whether the material was in the elastic or plastic range when the failure occurred.

The electrical strain-gage data were recorded by two automatic Gilmore strain plotters<sup>9\*</sup> and two Baldwin-Southwark Type L strain indicators. Figure 2 shows the arrangement of the testing apparatus used. The two Gilmore automatic strain plotters are in the foreground beside the recording deflectometer console. The Leeds-Northrup switch boxes and the Baldwin-Southwark strain indicators are on the platform of the 37-in. test chamber.

## TEST PROCEDURE AND RESULTS

Initial circularity plots were analyzed so that the initial out-of-roundness of the model could be determined for those stations recorded. The model stations were numbered from the open end. As shown in Figure 1, the odd-numbered stations were directly under a ring, and the even-numbered stations were on the shell midway between rings. The out-of-roundness at each station was determined by using the center-of-gravity and equivalent-circle methods. Results of the out-of-roundness analysis are tabulated in Table 1. Measurements were also made by Holt's method.<sup>10</sup> In this method, the initial out-of-roundness is the maximum deviation from a true circle in a given arc length. As applied to the circularity plots for the machined model, the out-of-roundness was negligible.

Deflectometer measurements were recorded at pressures of 100, 200, 300, 350, 370, 400, and 440 psi. As shown by a typical plot of the radial displacements at various pressure loadings (Figure 3), the model exhibited uniform radial displacement with no embryonic lobe formation. These results were substantiated by the strain-gage data.

Five different pressure runs were made during the test of Model BR-4A. The increments of pressure used during the various stages of the test are shown in Table 2, together with the pressures at which strains

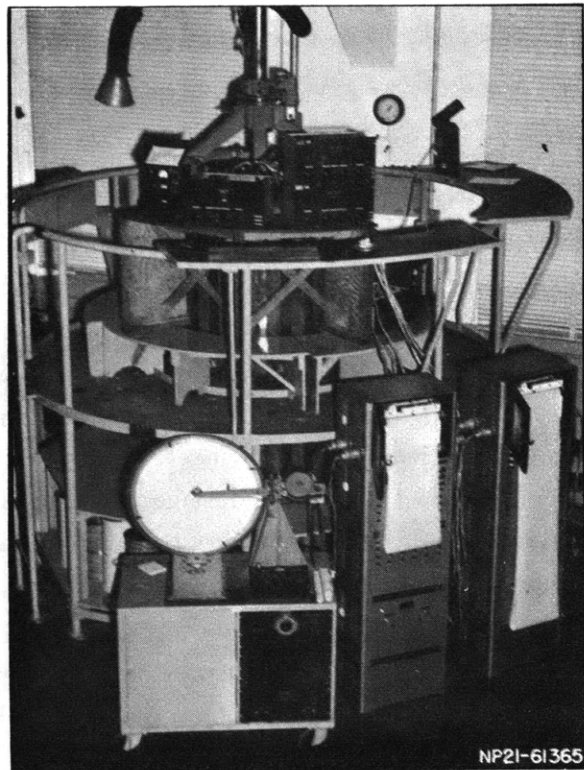


Figure 2 - Apparatus Used for Test of Model BR-4A

\*The Gilmore strain plotter, Model 114, is a 48-channel automatic strain-recording device. The record produced by this apparatus is a curve showing percent load versus percent strain for tension or compression. The ordinate or percent load is set manually and the percent strain is plotted automatically. The full-scale range of the percent-strain axis can be manually changed from 0.001 to 0.002 or 0.005.

TABLE 1

Ratios of Eccentricity to Shell Thickness for Stations Directly Under Rings and Midway Between Rings for Model BR-4A

| Model Stations | Ratio of Eccentricity to Shell Thickness ( $e/h$ ) |                          |
|----------------|--|--------------------------|
|                | Center-of-Gravity Method                           | Equivalent-Circle Method |
| 1 (Ring)       | 0.062  | 0.065                    |
| 2 (Bay)        | Strain-gage instrumentation in bay                 |                          |
| 3 (Ring)       | 0.060  | 0.071                    |
| 4 (Bay)        | 0.076  | 0.083                    |
| 5 (Ring)       | 0.059  | 0.068                    |
| 6 (Bay)        | 0.063  | 0.073                    |
| 7 (Ring)       | 0.047  | 0.054                    |
| 8 (Bay)        | 0.056  | 0.062                    |
| 9 (Ring)       | 0.035  | 0.039                    |

and radial displacements were recorded. There were no readings made at the failure pressure of 550 psi. The model withstood this pressure for approximately 2 min after which two lobes appeared between Stations 1 and 3 and three lobes appeared between Stations 3 and 5. The residual pressure with these five lobes (buckles) in the model was 318 psi. The pressure was then raised to 350 psi, and two more lobes formed between Stations 1 and 3 adjacent to the previously formed lobes. The pressure on the model then dropped to 305 psi, and the test was discontinued. The lobe spacing was such that 10 or 11 similar lobes could have formed around the circumference of the cylinder.

Figure 4 shows the damaged area on the inside of Model BR-4A after failure and Figure 5 shows the damaged area from the outside. These photographs indicate that the lobes in adjacent bays were staggered and that the ring between these bays deformed more or less sinusoidally. This has also been noticed in previous tests. The final collapse pattern for the welded (BR-4) and machined (BR-4A) models are shown in Figure 6. The welded model, BR-4 and the machined duplicate, BR-4A, failed by plastic shell instability at pressures of 390 and 550 psi, respectively. As previously noted, the staggered lobe formation is visible in both models.

The strain data collected during the test were essentially linear up to the pressure of 540 psi. This was true for all gages even though local yielding probably occurred around 530 psi at the outer fiber of the shell at midbay. A typical example of the recorded strain is shown in the pressure-strain plots in Figure 7.

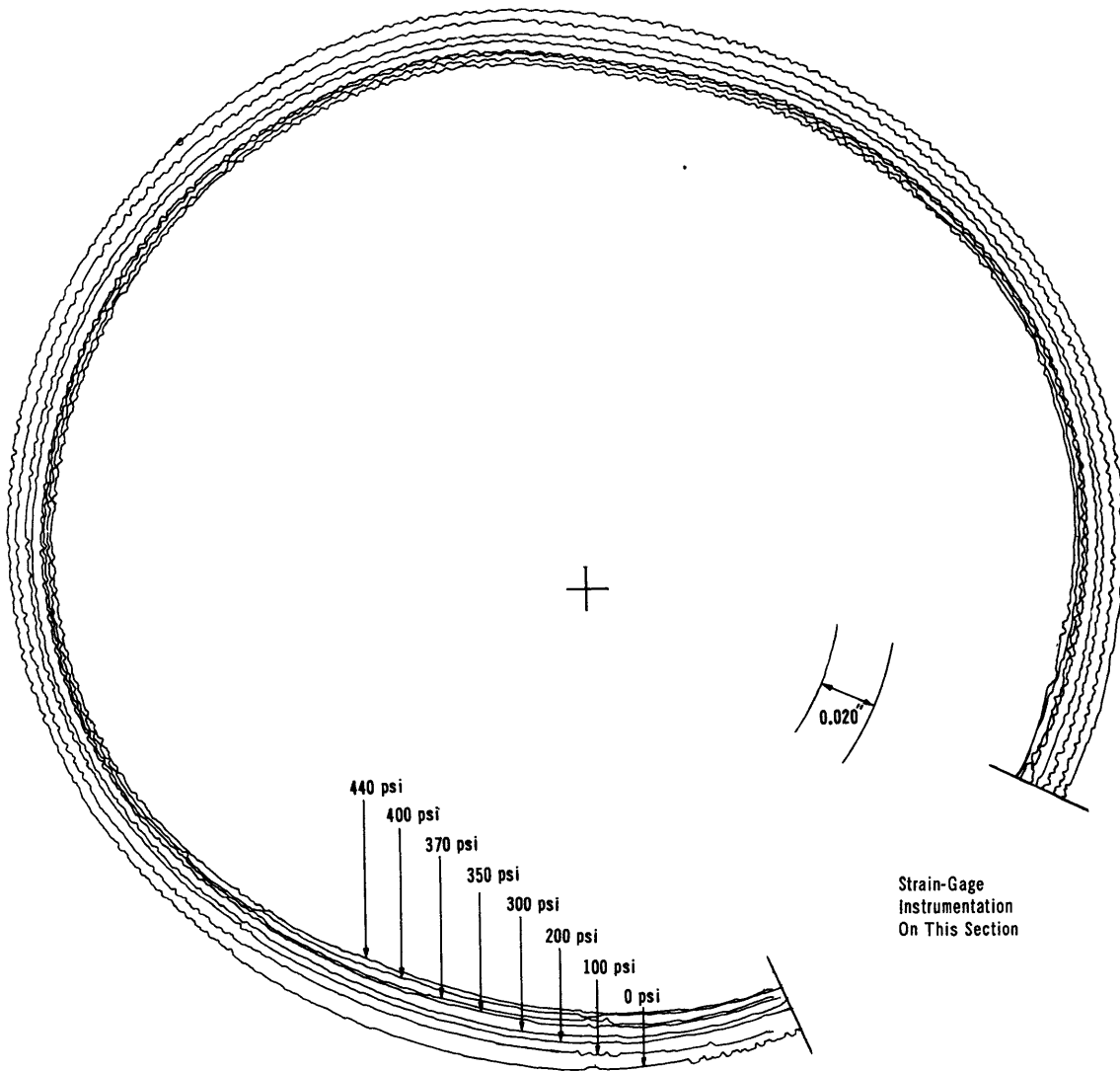


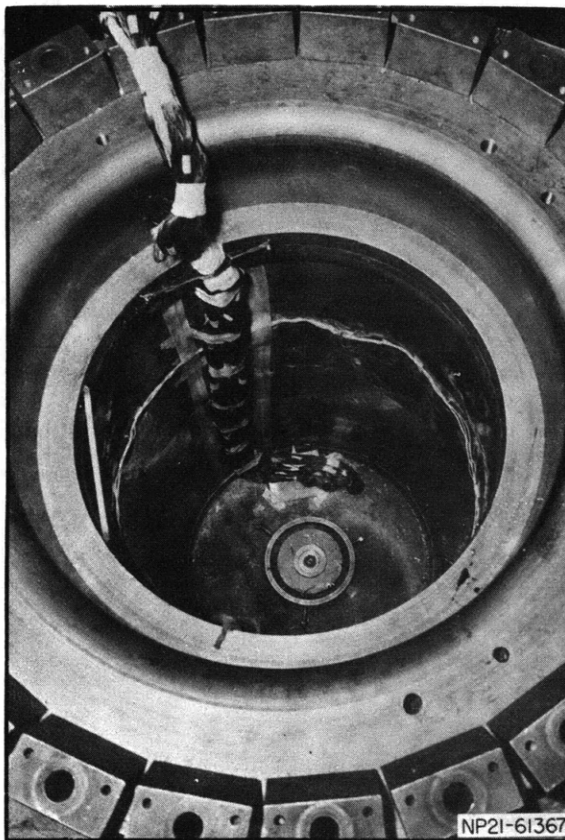
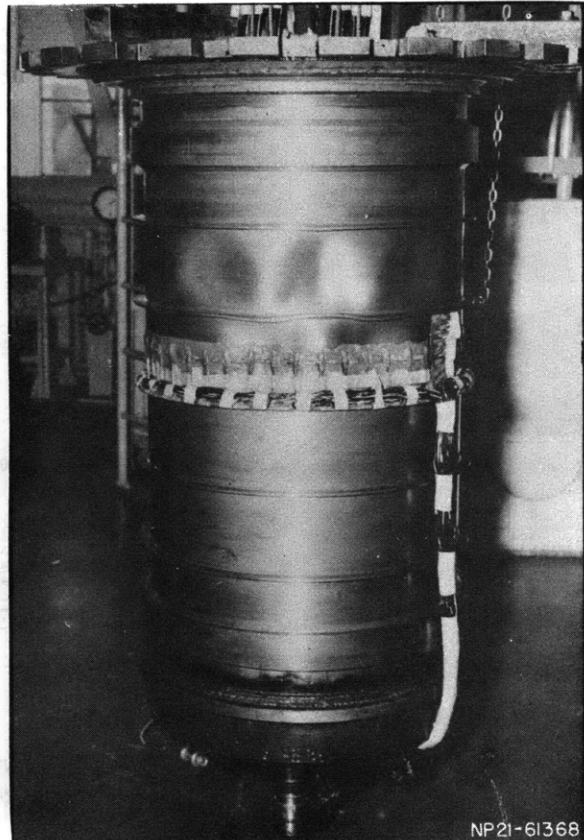
Figure 3 - Circularity Plot Showing Radial Displacements at Bay Midway Between Rings (Station 6)

TABLE 2

## Pressure Increments for Test of Model BR-4A

| Run 1           |                         |  | Run 2           |                         |  | Run 3           |                         |  | Run 4           |                         |  | Run 5           |                         |
|-----------------|-------------------------|--|-----------------|-------------------------|--|-----------------|-------------------------|--|-----------------|-------------------------|--|-----------------|-------------------------|
| Pressure<br>psi | Strain<br>Gages<br>Read | Stations at<br>Which Radial<br>Displacements<br>Were Taken | Pressure<br>psi | Strain<br>Gages<br>Read | Stations at<br>Which Radial<br>Displacements<br>Were Taken | Pressure<br>psi | Strain<br>Gages<br>Read | Stations at<br>Which Radial<br>Displacements<br>Were Taken | Pressure<br>psi | Strain<br>Gages<br>Read | Stations at<br>Which Radial<br>Displacements<br>Were Taken | Pressure<br>psi | Strain<br>Gages<br>Read |
| 0               | All                     | All  | 0               | All                     |  | 0               | All                     |  | 0               | All                     |  | 0               | All                     |
| 25              | Station 3               |  | 50              | All                     |  | 300             | All                     |  | 350             | All                     |  | 400             | All                     |
| 50              | All                     |  | 100             | All                     |  | 325             | Station 3               |  | 400             | All                     |  | 460             | All                     |
| 75              | Station 3               |  | 150             | All                     |  | 350             | All                     |  | 420             | All                     |  | 500             | All                     |
| 100             | All                     | All  | 200             | All                     |  | 370             | All                     | All  | 440             | All                     | All*   | 510             | All                     |
| 125             | Station 3               |  | 225             | Station 3               |  | 390             | All                     |  | 460             | All                     |  | 520             | All                     |
| 150             | All                     |  | 250             | All                     |  | 400             | All                     | All  | 480             | All                     |  | 530             | All                     |
| 175             | Station 3               |  | 275             | Station 3               |  | 250             | All                     |  | 500             | All                     |  | 540             | All                     |
| 200             | All                     | All  | 300             | All                     | All  | 0               | All                     |  | 0               | All                     |  | 550             | Failure                 |
| 0               | All                     |  | 325             | Station 3               |  |                 |                         |  |                 |                         |  |                 |                         |
|                 |                         |  | 350             | All                     | All  |                 |                         |  |                 |                         |  |                 |                         |
|                 |                         |  | 0               | All                     |  |                 |                         |  |                 |                         |  |                 |                         |

\*Recording deflectometer removed from model after these readings were taken.

Figure 4 - Internal View of Model BR-4A  
After FailureFigure 5 - External View of Model BR-4A  
After Failure

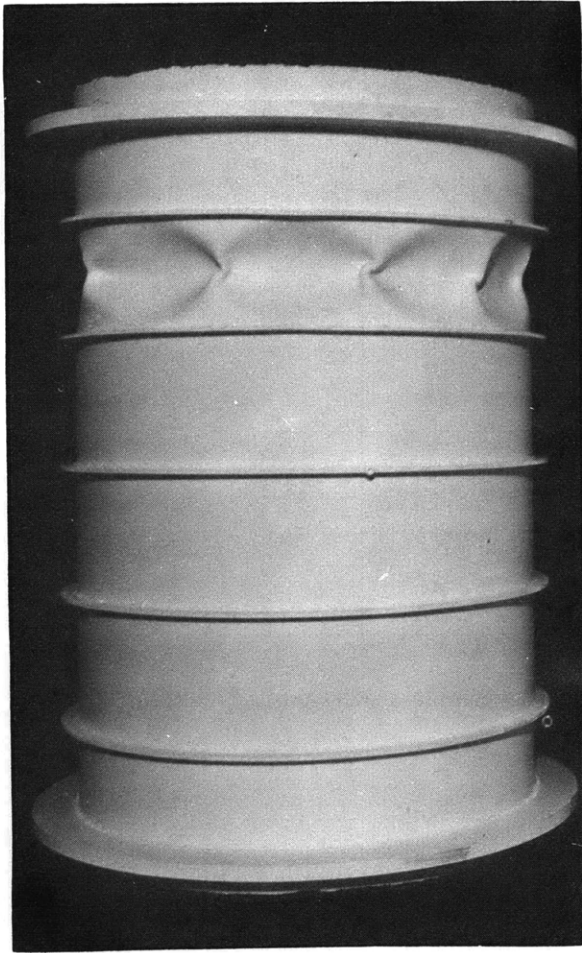


Figure 6a - Model BR-4

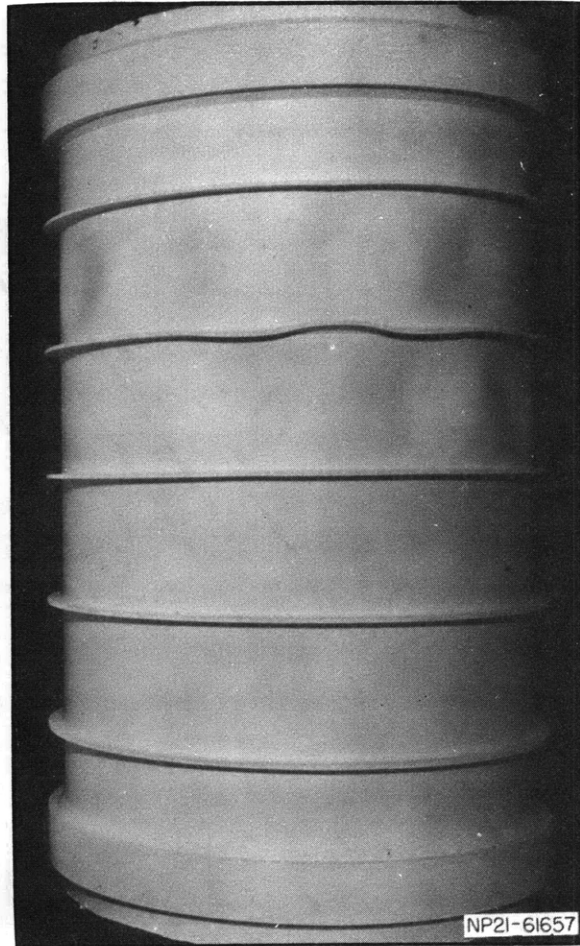


Figure 6b - Model BR-4A

Figure 6 - Exterior View of Final Collapse Pattern of Models BR-4 and BR-4A

Figure 7a has five pressure runs with corresponding strains plotted on the same coordinate system with their origins offset by  $100 \mu$  in/in. Since the strains were linear for each loading, this strain scale was used for convenience and ease in comparing the data. Figure 7b is a plot of the maximum longitudinal and circumferential strain on the outside of the shell at midbay. Figure 7c shows the internal longitudinal and circumferential strains on the shell adjacent to a reinforcing ring.

The linearity and agreement in the strain sensitivity for successive runs, as illustrated in Figure 7, was typical for all electrical strain gages that functioned properly.

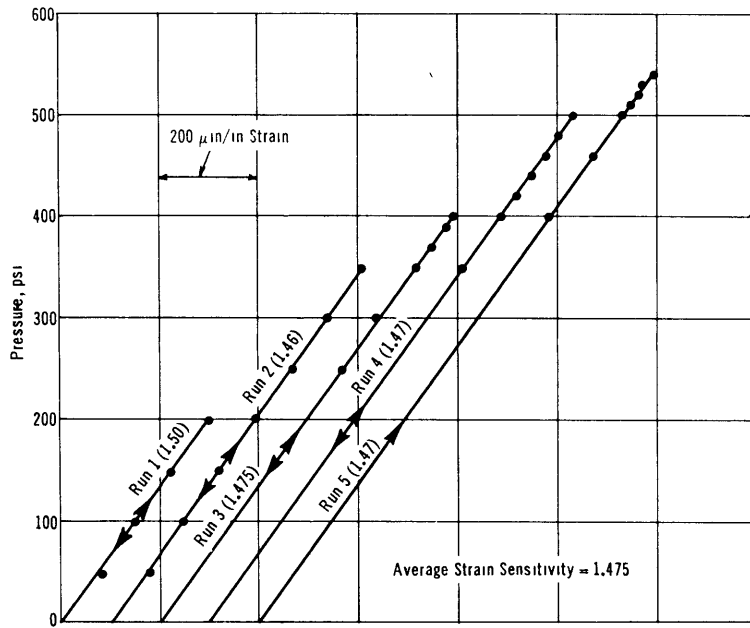


Figure 7a - Circumferential Strain on Outer Fiber of Reinforcing Ring

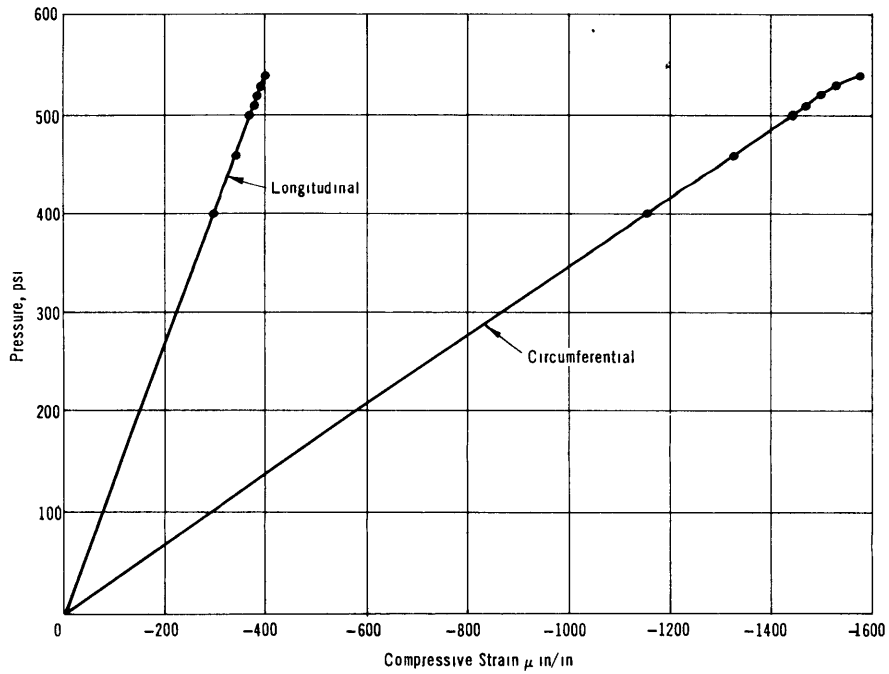


Figure 7b - External Longitudinal and Circumferential Strain on the Shell at Midbay

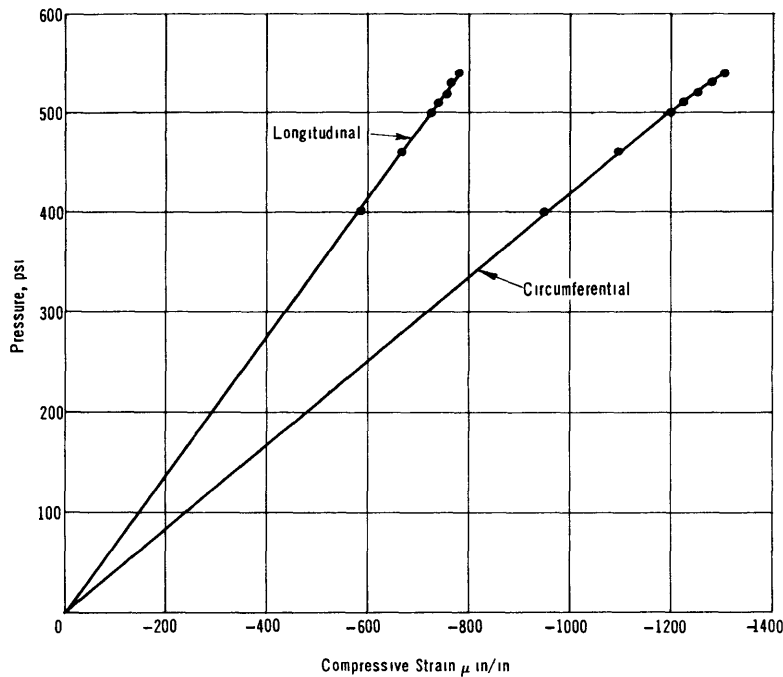


Figure 7c - Internal Longitudinal and Circumferential Strain on Shell Adjacent to Reinforcing Ring  
 Figure 7 - Linear Variation of Strain with Pressure at Successive Pressure Loadings

## DISCUSSION OF RESULTS

### DEFLECTIONS

The deflection pattern shown in Figure 3 indicates that the model deformed uniformly in the radial direction. The measured strain sensitivities shown in Figures 8 and 9 are plots of the strain sensitivities for the longitudinal and circumferential gages at Station 4. The uniformity of these sensitivities indicates an absence of embryonic lobe formations and uniform deformation of the model.

Values of the mean inward radial displacement per unit pressure at the rings and midbay, recorded by electrical strain gages and the automatic recording deflectometer, are tabulated in Table 3 together with values computed from the theory of Salerno and Pulos. The average inward radial displacement measured by the deflectometer was 0.000039 in. per unit pressure midway between the rings and 0.000021 in. per unit pressure at the rings. From the recorded strains, the mean radial displacement was computed to be 0.000041 in. per unit pressure midway between the rings and 0.000018 in. per unit pressure at the rings. Thus the displacements predicted by the Salerno and Pulos theory<sup>7</sup> are 1.025 and 0.818 times the values determined from the circumferential strain gages and 0.975 and 0.955 times the values determined from the deflectometer charts midway between the rings and at the rings, respectively.

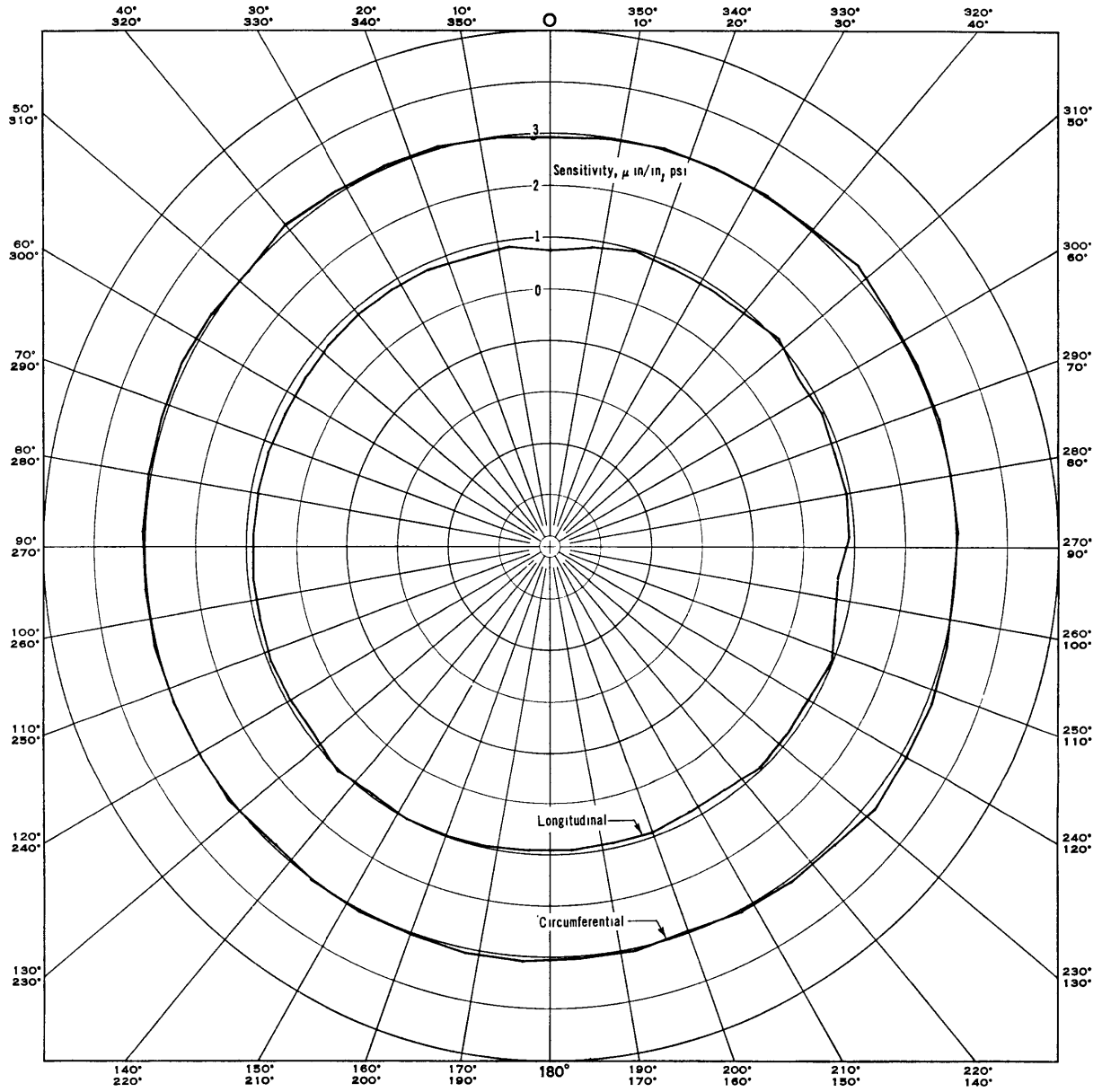


Figure 8 - Strain Sensitivities at Outer Surface of Station 4 at Midbay

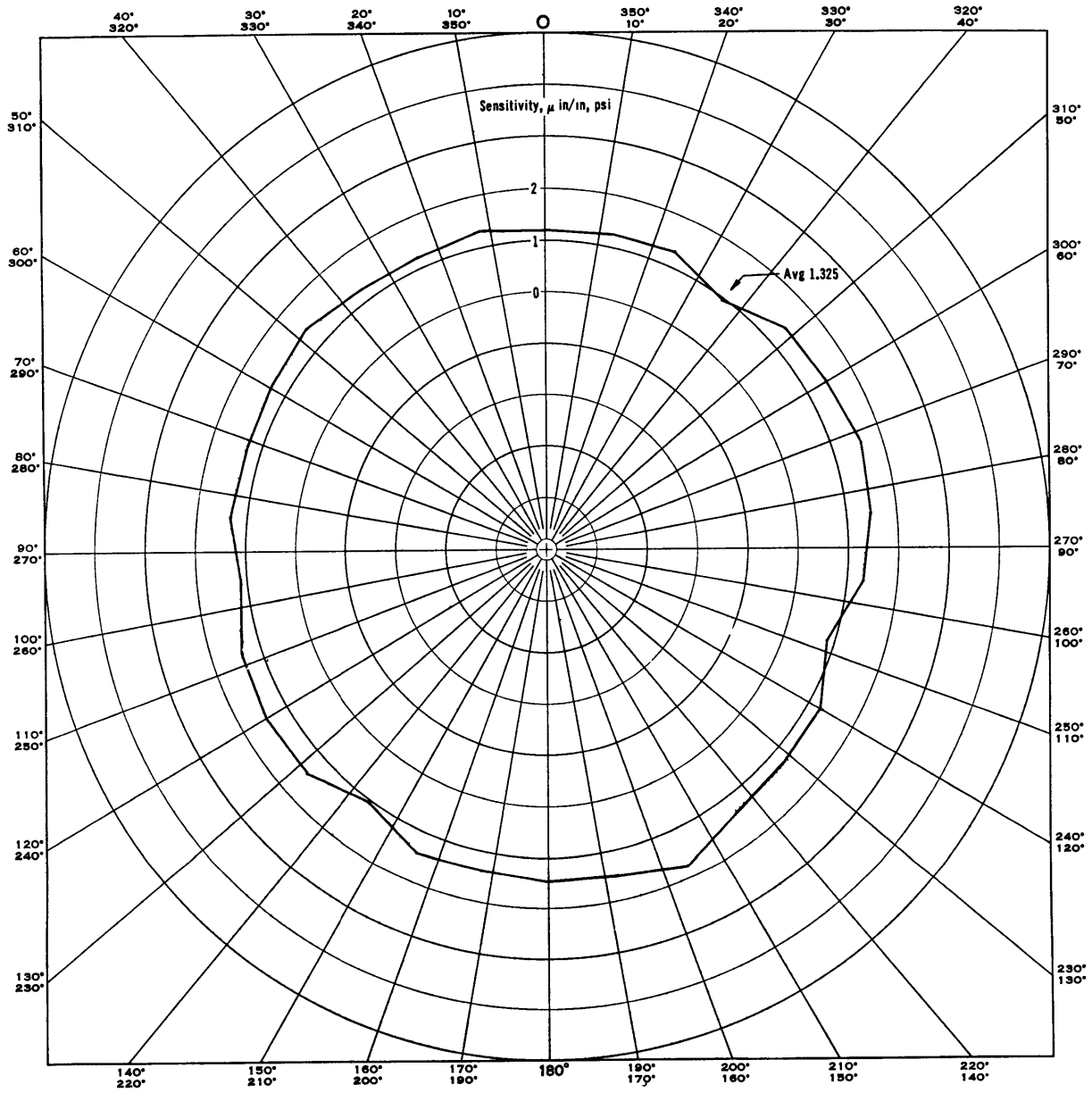


Figure 9 - Circumferential Strain Sensitivities on the Outer Surface of Ring at Station 5

TABLE 3

Comparison of Theoretical and Experimental Radial Displacement for Model BR-4A

|                              | Displacement per psi, in. |              |
|------------------------------|---------------------------|--------------|
|                              | Midway Between Rings      | At the Rings |
| Salerno-Pulos Theory         | 0.000040                  | 0.000022     |
| Circumferential Strain Gages | 0.000041                  | 0.000018     |
| Recording Deflectometer      | 0.000039                  | 0.000021     |

## STRAINS

The elastic theories of von Sanden and Gunther<sup>8</sup> and Salerno and Pulos<sup>7</sup> make it possible to compute the stresses and strains in ring-stiffened cylindrical shells subjected to hydrostatic pressure. Each theory assumes that Hooke's law is valid and that elastic buckling of the structure has not taken place. Plots showing the relationship of the two theories for Model BR-4A are presented in Figure 10. It is evident from this comparison that both theories furnish a linear relationship between pressure and stress for this model. Because of this linearity, the strain sensitivities (strain per unit pressure) may be used as a more convenient method of comparing theoretical and experimental results.

The longitudinal and circumferential strain sensitivities midway between the rings on the outer surface of the shell computed by the theory of Salerno and Pulos<sup>7</sup> are 0.78 and 2.98  $\mu\text{in/in/psi}$ , respectively. The strain sensitivities in Figure 8 agree fairly well with these values. Figure 9 shows the circumferential strain sensitivities at the outer fiber of the ring at Station 5. Even though these sensitivities are more erratic than those shown in Figure 8, they do not indicate any regular bending pattern. In fact, with the exception of five gages, the sensitivities are quite uniform.

The theoretical and experimental distributions of circumferential strain sensitivity are shown in Figure 11. The internal strain sensitivities showed very good agreement with theory. However, three of the external circumferential strain gages gave results which appear to be in error. Therefore, the results from the circumferential distribution of gages on the outer surface are not presented. The experimental longitudinal strain sensitivities at the inner and outer surfaces of the shell are plotted in Figure 12. As shown by these curves, the agreement between experiment and theory is good.

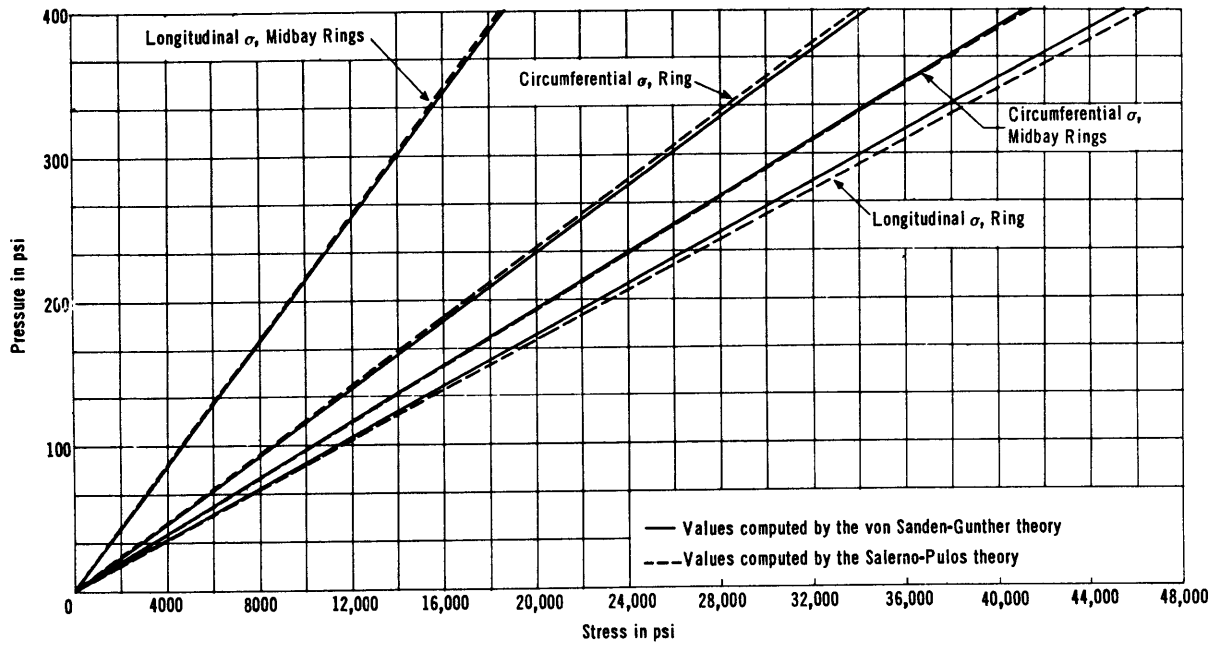


Figure 10 - Variation of Stress at Interior of Shell with Pressure

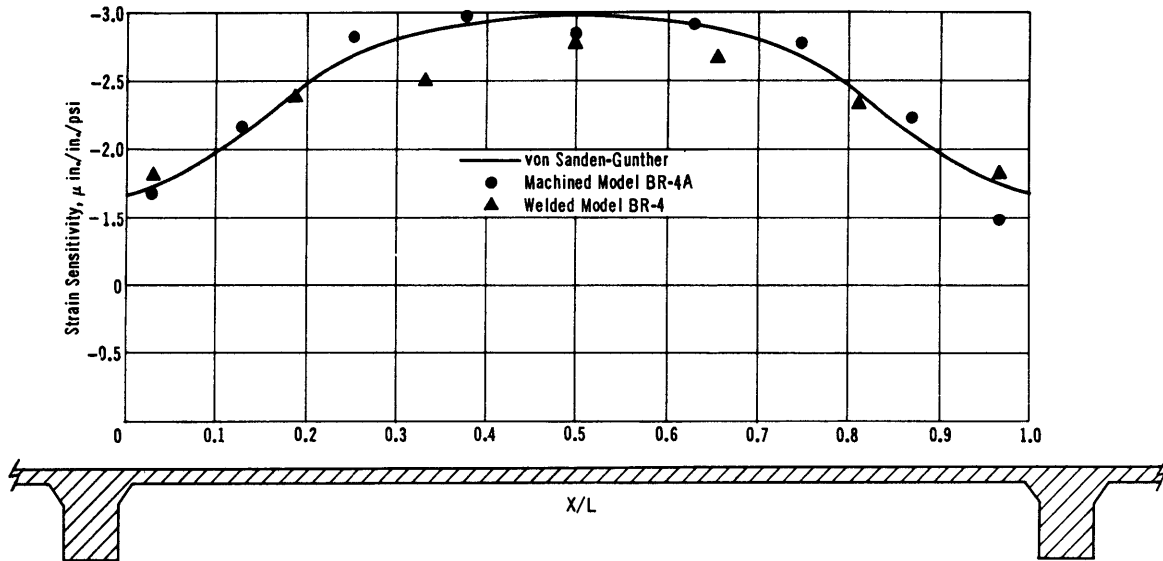


Figure 11 - Theoretical and Experimental Distribution of Circumferential Strain Sensitivity

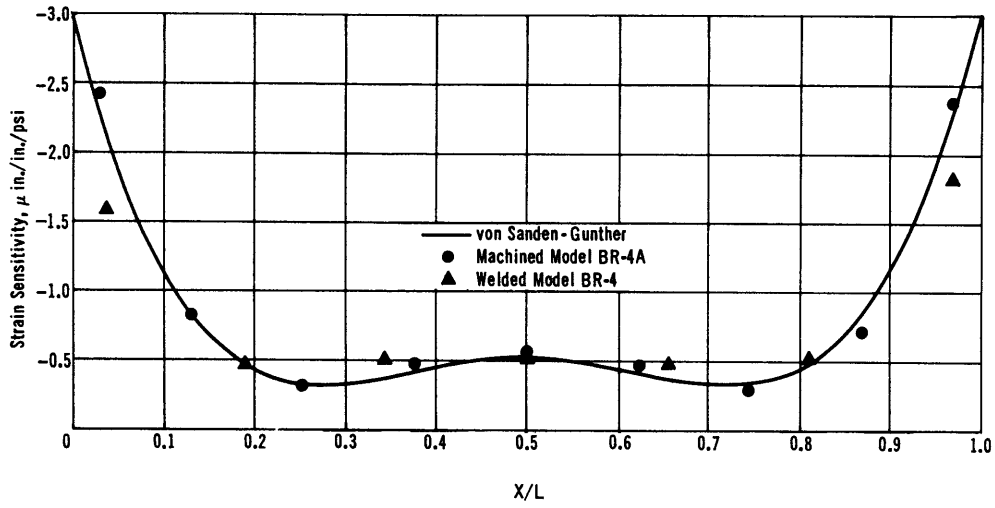


Figure 12a - Internal Strain Sensitivity

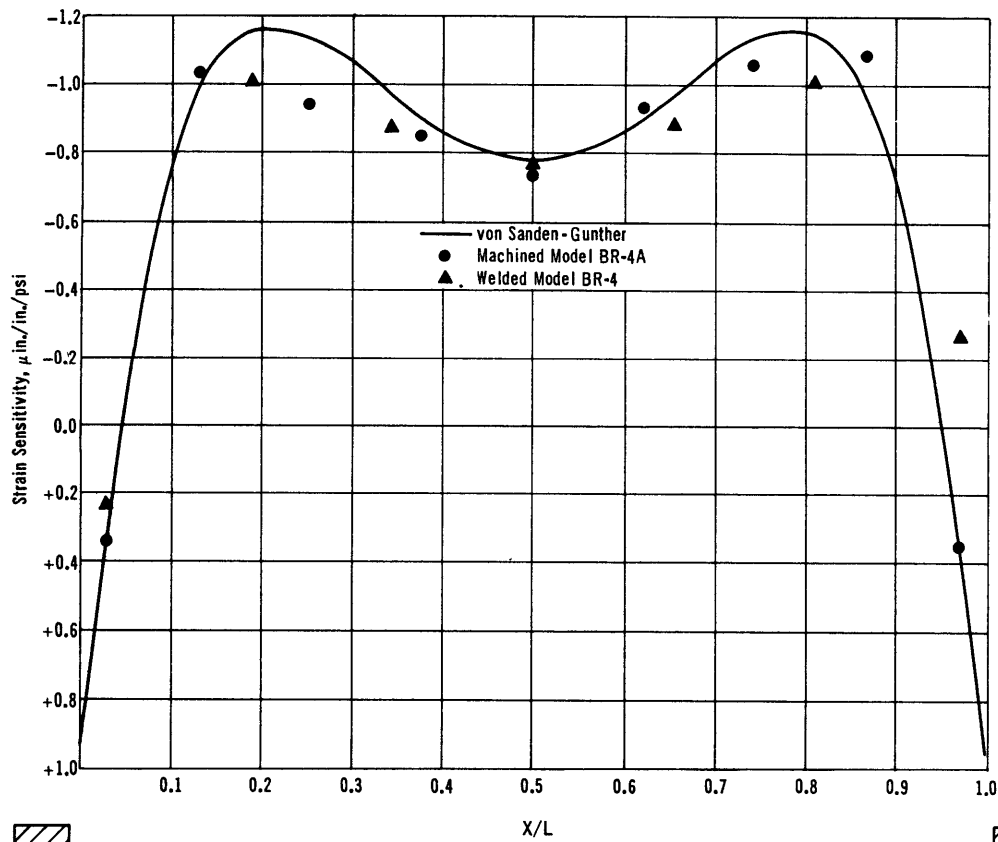


Figure 12b - External Strain Sensitivities

Figure 12 - Theoretical and Experimental Distribution of Longitudinal Strain Sensitivity

## COLLAPSE PRESSURE

The elastic shell-instability pressure for a perfect cylindrical shell with the geometry of Models BR-4 and BR-4A as predicted by the von Mises theory<sup>11</sup> was 610 psi with a buckling configuration of ten lobes. Additional calculations were made using the shell-instability theories of Nash<sup>12</sup> (Case II, Elastic Support) and Salerno and Levine<sup>13,14</sup> (Case II, Rigid Support and Case III, Elastic Support). These theoretical buckling pressures are tabulated in Table 4.

The Hencky-von Mises theory of failure<sup>15</sup> using the von Sanden-Gunther<sup>8</sup> stresses at the median surface of the shell midway between the rings predicted a shell yield strength of 551 psi. This pressure for axisymmetric yielding of the shell plating was lower than those obtained from the available buckling theories listed in Table 4. With a  $\lambda$  of 1.103, it was expected that the machined model might fail close to the axisymmetric yield value. Thus a plastic shell-instability type of failure, initiated by local yielding, was not unexpected. In the transition range ( $0.8 < \lambda < 1.2$ ), it is expected that models may fail by axisymmetric yielding in the shell, by plastic shell instability, or by elastic shell instability.

The machined Model BR-4A failed at a pressure of 550 psi with the formation of lobes in the shell plating. Since most of the shell eccentricity had been eliminated in this model, it seems that the difference between the collapse pressure and the theoretical buckling pressure was not due entirely to the minute initial imperfections. Therefore, collapse was probably due to local yielding of the shell material followed by plastic shell instability. Since this model was thus in the transition range between shell yield and elastic shell instability, the results are inconclusive in that they could not be used to evaluate either theory of failure.

TABLE 4

Collapse Pressures for Model BR-4A According to Various Theories of Shell Instability

| Theory                   | Predicted Pressure<br>psi | Predicted No.<br>of Lobes (n) |
|--------------------------|---------------------------|-------------------------------|
| von Mises                | 610                       | 10                            |
| Salerno-Levine, Case II  | 865                       | 10                            |
| Salerno-Levine, Case III | 781                       | 10                            |
| Nash, Case III           | 823                       | 12                            |

## MODEL COMPARISON

In comparing the test results of Models BR-4 and BR-4A, it must be kept in mind that BR-4 was a fabricated model which had initial imperfections in the shell and reinforcing rings, due to out-of-roundness and residual stresses. Model BR-4A on the other hand was a machined and stress-relieved model that was as nearly perfect as modern machining and metallurgical processes could make it.

Both models had a thinness factor  $\lambda$  of 1.103 because the geometries and even the average yield strengths of the material were the same. However, Model BR-4 collapsed at a pressure of 390 psi giving a pressure factor  $\psi$  of 0.78, while Model BR-4A collapsed at 550 psi giving a  $\psi$  of 1.101. The difference of 160 psi in the collapse pressures can be attributed to the initial out-of-roundness and the residual rolling and welding stresses in the fabricated model BR-4.

As shown in Figures 11 and 12, the strain sensitivities for both models check the elastic theory of von Sanden-Gunther. In addition, there is very little difference between the strain sensitivities of the welded and machined cylinders. However, there are discrepancies between the experimental points in the area near the rings. In the machined cylinder the ring-shell combination was a homogeneous section; the welds were simulated, but there would be no residual stresses or distortion in that area. The fabricated BR-4 had a ring-shell combination which did not constitute a homogeneous section, and there was residual distortion caused by welding, as evidenced by the initial circularity plots of Model BR-4. The greatest measured difference in radii between a ring (Station 3) and adjacent bay (Station 4) was 0.017 in.; however, the greater portion of this distortion was localized at the weld. It appears, therefore, that the initial distortion in the welded area was the cause of the discrepancy in the strain sensitivities.

For both models, the mean radial displacements determined from the deflectometer plots and the recorded experimental strains at the rings and midway between the rings were in good agreement with those predicted by the theory of Salerno-Pulos. These values are tabulated in Table 5.

TABLE 5

Comparison of Theoretical and Experimental Radial Displacements for Machined Model BR-4A and Welded Model BR-4

| Determination of Displacement | Displacement per psi, inches |          |              |          |
|-------------------------------|------------------------------|----------|--------------|----------|
|                               | Midway Between Rings         |          | At the Rings |          |
|                               | BR-4A                        | BR-4     | BR-4A        | BR-4     |
| Theory of Salerno-Pulos       | 0.000040                     | 0.000040 | 0.000022     | 0.000022 |
| Circumferential Strain Gages  | 0.000041                     | 0.000035 | 0.000018     | 0.000024 |
| Recording Deflectometer       | 0.000039                     | 0.000044 | 0.000021     | 0.000026 |

## CONCLUSIONS

1. The machined Model BR-4A failed at a pressure of 550 psi with lobes corresponding to a possible 10- or 11-lobe buckling configuration. The buckling configuration was probably precipitated by local yielding of the shell material; therefore, the failure could be regarded as due to plastic shell instability.

2. The lower collapse pressure of the welded model BR-4 (390 psi) can be attributed to the initial eccentricity and the residual stresses present in the fabricated model.

3. The elastic buckling pressures predicted by the theories of von Mises (610 psi), Salerno and Levine (781 psi), and Nash (823 psi) were all greater than the actual collapse pressure of 550 psi. The failure pressure predicted by the axisymmetric yield criterion of Hencky and von Mises using the von Sanden and Gunther stresses at the median surface of the shell midway between rings was 551 psi.

4. The results from this test cannot be used to check theory either for a elastic shell instability or for axisymmetric shell yield because the model failed by plastic shell instability with the formation of circumferential lobes.

5. The measured strains for the machined Model BR-4A were nearly linear up to the collapse pressure. No embryonic lobe formations were detected by the strain gage results or by the radial displacement contours. However, embryonic lobe formations were evident in the fabricated BR-4 in the form of accentuated initial out-of-roundness deformations.

6. The strain distributions given by the elastic theories of von Sanden and Gunther and of Salerno and Pulos were in good agreement with the initial measured strains.

From the close agreement noticed in this experimental investigation, it appears that these two theories can be considered adequate and valid.

## RECOMMENDATIONS

1. Machined models should be tested in the range that is of interest to designers of pressure vessels and submarines, in order to study separately the effects of initial out-of-roundness and residual stresses.

2. Additional tests should be made on duplicate welded and machined reinforced cylindrical shells designed to fail by elastic shell instability. These tests could be used to determine the effects of initial out-of-roundness and of residual welding and rolling stresses, as well as to verify experimentally the adequacy of existing buckling theories.

## ACKNOWLEDGMENT

The authors would like to thank Mr. R.F. Keefe for help rendered during the instrumentation and testing of the model.

## REFERENCES

1. Windenburg, D.F. and Trilling, C., "Collapse by Instability of Thin Cylindrical Shells under External Pressure," Transaction of the American Society of Mechanical Engineers, Vol. 56, No. 11 (1934), David Taylor Model Basin Report 385 (Jul 1934).
2. Nash, W.A. and Wenk, E., Jr., "Tests of the Elastic Stability of a Ring-Stiffened Cylindrical Shell, Model BR-1 ( $\lambda = 1.82$ ), Subjected to Hydrostatic Pressure," David Taylor Model Basin Report C-439 (Mar 1953) CONFIDENTIAL.
3. Slankard, R.C. and Nash, W.A., "Tests of the Elastic Stability of a Ring-Stiffened Cylindrical Shell, Model BR-5 ( $\lambda = 1.705$ ), Subjected to Hydrostatic Pressure," David Taylor Model Basin Report 822 (May 1953).
4. Slankard, R.C., "Test of the Elastic Stability of a Ring-Stiffened Cylindrical Shell, Model BR-4 ( $\lambda = 1.103$ ) Subjected to Hydrostatic Pressure," David Taylor Model Basin Report 876 (Feb 1955).
5. Slankard, R.C. and Galletly, G.D., "General Instability of Machined Ring-Stiffened Cylindrical Shells Subjected to External Hydrostatic Pressure," David Taylor Model Basin Report (in preparation).
6. Keefe, R.F. and Slankard, R.C., "The Effect of Bulkhead Spacing on the General Instability Strength of Machined Stiffened Cylindrical Shells," David Taylor Model Basin Report (in preparation).
7. Salerno, V.L. and Pulos, J.G., "Stress Distribution in a Circular Cylindrical Shell under Hydrostatic Pressure Supported by Equally Spaced Circular Ring Frames," Polytechnic Institute of Brooklyn, Aero Lab Report 171-A (1951).
8. von Sanden, K. and Gunther, K., "The Strength of Cylindrical Shells Stiffened by Frames and Bulkheads, under Uniform External Pressure on all Sides," (Uber das Festigkeits problem Querversteifter Hohlzylinder unter Allseitig Gleichmassigem Aussendruck) Werft and Reederei, Vol. 1 (1920), Nos. 8, 9, and 10 and Vol. 2 (1921) No. 17 (TMB Translation 38 March 1952).
9. Carleton, R.J. Jr., "High Speed Data Plotting Instrument for Strain Gages," Instrument Society of America, Vol. 1, No. 10, pp 21-24 (October 1954).
10. Holt, M., "A Procedure for Determining the Allowable Out-of-Roundness for Vessels under External Pressure," Transactions of the American Society of Mechanical Engineers, Vol. 74, No. 7 (1952).
11. von Mises, R., "Der kritische Aussendruck fur allseits belastete zylindrische Rohre," Fest. Zum 70 Geburtstage, von Prof. Dr. A. Stodola, Zurich (1929) pp. 418-430.
12. Nash, W.A., "Buckling of Multi-Bay Ring-Reinforced Cylindrical Shells Subject to Hydrostatic Pressure," Journal of Applied Mechanics, Vol. 20, No. 4, (Dec 1953) pp 469-474. (Also David Taylor Model Basin Report 785 (Apr 1954).

13. Salerno, V.L. and Levine, B., "Buckling of Circular Cylindrical Shells with Evenly Spaced Equal Strength Circular Ring Frames, Part II," Polytechnic Institute of Brooklyn, Aero Lab Report 169 (1950).
14. Salerno, V.L. and Levine, B., "The Determination of the Hydrostatic Buckling Pressure for Circular Cylindrical Shells Reinforced with Rings," Polytechnic Institute of Brooklyn, Aero Lab Report 182 (1951).
15. Murphy, G., "Advanced Mechanics of Materials," McGraw-Hill Book Co., Inc., New York (1946) pp 76-84.



## INITIAL DISTRIBUTION

## Copies

14 Chief, BuShips, Library (Code 312)  
 5 Tech Library  
 1 Tech Asst to Chief of Bureau (Code 106)  
 2 Prelim Design (Code 420) (421)  
 1 Ship Pro, Underwater Expl Res, etc. (Code 423)  
 1 Hull Design (Code 440)  
 2 Sci-Struc & Hydro (Code 442)  
 2 Submarines (Code 525)

2 CHONR, Mech Br (Code 438)

2 CDR, USNOL

1 DIR, USNRL

2 CDR, Norfolk Naval Shipyard, UERD (Code 270)

2 CDR, Portsmouth Naval Shipyard

2 CDR, Mare Island Naval Shipyard

3 SUPSHIPINSORD, Groton, Conn.

1 CO & DIR, USNEES, Annapolis, Md.

1 CDR, USNOTS, China Lake, Calif.

1 CO, USNUOS, Newport, R.I.

1 Chief, AFSWP, Washington, D.C.

1 DIR, Langley Aero Lab, Langley Field, Va.

1 CG, Hdqtrs, Air Materiel Command, Wright-Patterson AFB, O.

2 Asst Secy of Defense (Research and Development)

1 Prof. Jesse Ormondroyd, Dept of Engin Mech, Univ of Michigan, Ann Arbor, Mich.

1 Dr. N.J. Hoff, Head, Dept of Aero Engin and Appl Mech, Polytech Inst of Brooklyn; Brooklyn, N.Y.

1 DR. J.N. Goodier, School of Engin, Stanford Univ, Stanford, Calif.

1 Dr. F.K. Teichmann, Dept of Aero Engin, New York Univ, New York, N.Y.

1 Dr. E. Sternberg, Illinois Inst of Tech, Tech Ctr, Chicago, Ill.

1 Dr. W. Prager, Chairman, Grad Div of Appl Math, Brown Univ, Providence, R.I.

1 Dr. W.H. Hoppmann, II, Dept of Appl Mech, Johns Hopkins Univ, Baltimore, Md.

1 Prof. R.M. Hermes, College of Engin, Univ of Santa Clara, Santa Clara, Calif.

1 Dr. R.P. Petersen, DIR, Appl Physics Div, Sandia Lab, Albuquerque, N. Mex.

1 Dr. F.H. Clauser, Chairman, Dept of Aero, Johns Hopkins Univ, Baltimore, Md.

1 Prof. Lloyd Donnell, Dept of Mech, Illinois Inst of Tech, Tech Ctr, Chicago, Ill.

1 Dr. Bruce Johnson, Prof. of Struct Engin, Dept of Civil Engin, Univ of Michigan, Ann Arbor, Mich.

1 Dr. N.M. Newmark, Struct Res Div, College of Engin, Univ of Illinois, Urbana, Ill.

## Copies

1 Prof. T.J. Dolan, Dept of Theoretical and Appl Mech, Univ of Illinois, Urbana, Ill.

1 Dr. R.D. Mindlin, Columbia Univ, New York, N.Y.

1 Dr. F.V. Hartman, The Aluminum Ore Co, E. St. Louis Mo.

1 Dr. Rolland G. Sturm, Dir, Auburn Res Fdtn & Exp Stn, Alabama Polytech Inst, Auburn, Ala.

1 Prof. Everett O. Waters, Dept of Mech Engin, Yale Univ, New Haven, Conn.

1 Dr. M. Hetényi, Northwestern Univ, Tech Inst, Evanston, Ill.

1 Mr. Harry C. Boardman, Dir of Res, Chicago Bridge and Iron Co, Chicago, Ill.

1 Mr. W.R. Burrows, Asst Chief Engr, Whiting Refinery, Standard Oil Company (Indiana), Whiting, Ind.

1 Mr. M.B. Higgins, Supervising Engr, The Texas Co, New York, N.Y.

1 Dr. Marshall Holt, Aluminum Res Lab, New Kensington, Pa.

1 Mr. E.C. Korten, Hartford Steam Boiler Insp & Ins Co, Hartford, Conn.

1 Mr. H.L. O'Brien, Graver Tank & Mfg Co, E. Chicago, Ind.

1 Mr. D.B. Wesstrom, Des Div, Engin Dept, E.I. duPont de Nemours & Co, Wilmington, Del.

1 Applied Physics Lab, Johns Hopkins Univ, Silver Spring, Md.

1 The Babcock & Wilcox Co, Res & Dev Dept, Alliance, O.

3 Pressure Vessel Research Committee, New York, N.Y.

1 Dr. James R. Adams, Dev Engr, Midvale Cdg, Philadelphia, Pa.

1 Mr. Perry R. Cassidy, The Babcock & Wilcox Co, Boston, Mass.

1 Mr. Harold O. Hill, Asst Chief Engr, Fabricated Steel Construction, Bethlehem Steel Co, Bethlehem, Pa.

1 Mr. Henry Liessenberg, Stress Res Engr, Combustion Engineering, Inc, New York, N.Y.

1 Mr. James J. Murphy, Section Engr, Dev Div, M.W. Kellogg Co, New York, N.Y.

1 Mr. Cyril O. Rhys, Sr., Independent Consultant, Westfield, N.J.

1 Mr. G.J. Schoessow, The Babcock & Wilcox Co, Barberton, O.

1 Mr. W. Spraragen, DIR, Welding Res Council, New York, N.Y.

1 Mr. George W. Watts, Dir of Engin, Standard Oil Co (Indiana) Chicago, Ill.

9 BJSM (NS)

1 British Shipbldg Res Assn, London, W.1, England

8 ALUSNA, London, England



**David W. Taylor Model Basin. Rept. 997.**

AN EXPERIMENTAL INVESTIGATION OF THE SHELL-INSTABILITY STRENGTH OF A MACHINED, RING-STIFFENED CYLINDRICAL SHELL UNDER HYDROSTATIC PRESSURE (MODEL BR-4A), by Arthur F. Kirstein and Robert C. Slankard. Apr. 1956. iii, 23 p. incl. figs., tables, refs. (Research and development report)

The effects of initial eccentricity and residual welding and rolling stresses on the buckling strength of a stiffened cylinder were investigated by tests of a machined and stress-relieved model, Model BR-4A, identical in size and material with a previously tested fabricated model, Model BR-4. The experimental collapse pressure of 550 psi for Model BR-4A agrees well with collapse pressures predicted by theory and, when compared with the collapse pressure of 390 psi for Model BR-4, indicates that initial eccentricity and residual stresses have a decided effect on the strength under external hydrostatic pressure.

1. Cylindrical shells (Stiffened) – Stability – Measurement
2. Cylindrical shells (Stiffened) – Stresses – Measurement
  - I. Kirstein, Arthur F.
  - II. Slankard, Robert C.
  - III. NS 731-038

**David W. Taylor Model Basin. Rept. 997.**

AN EXPERIMENTAL INVESTIGATION OF THE SHELL-INSTABILITY STRENGTH OF A MACHINED, RING-STIFFENED CYLINDRICAL SHELL UNDER HYDROSTATIC PRESSURE (MODEL BR-4A), by Arthur F. Kirstein and Robert C. Slankard. Apr. 1956. iii, 23 p. incl. figs., tables, refs. (Research and development report)

The effects of initial eccentricity and residual welding and rolling stresses on the buckling strength of a stiffened cylinder were investigated by tests of a machined and stress-relieved model, Model BR-4A, identical in size and material with a previously tested fabricated model, Model BR-4. The experimental collapse pressure of 550 psi for Model BR-4A agrees well with collapse pressures predicted by theory and, when compared with the collapse pressure of 390 psi for Model BR-4, indicates that initial eccentricity and residual stresses have a decided effect on the strength under external hydrostatic pressure.

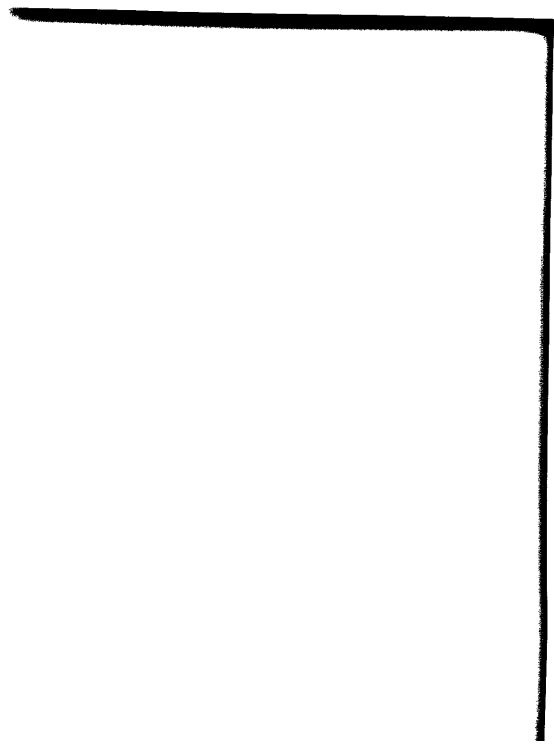
1. Cylindrical shells (Stiffened) – Stability – Measurement
2. Cylindrical shells (Stiffened) – Stresses – Measurement
  - I. Kirstein, Arthur F.
  - II. Slankard, Robert C.
  - III. NS 731-038

**David W. Taylor Model Basin. Rept. 997.**

AN EXPERIMENTAL INVESTIGATION OF THE SHELL-INSTABILITY STRENGTH OF A MACHINED, RING-STIFFENED CYLINDRICAL SHELL UNDER HYDROSTATIC PRESSURE (MODEL BR-4A), by Arthur F. Kirstein and Robert C. Slankard. Apr. 1956. iii, 23 p. incl. figs., tables, refs. (Research and development report)

The effects of initial eccentricity and residual welding and rolling stresses on the buckling strength of a stiffened cylinder were investigated by tests of a machined and stress-relieved model, Model BR-4A, identical in size and material with a previously tested fabricated model, Model BR-4. The experimental collapse pressure of 550 psi for Model BR-4A agrees well with collapse pressures predicted by theory and, when compared with the collapse pressure of 390 psi for Model BR-4, indicates that initial eccentricity and residual stresses have a decided effect on the strength under external hydrostatic pressure.

1. Cylindrical shells (Stiffened) – Stability – Measurement
2. Cylindrical shells (Stiffened) – Stresses – Measurement
  - I. Kirstein, Arthur F.
  - II. Slankard, Robert C.
  - III. NS 731-038



MIT LIBRARIES DUPL  
  
3 9080 02754 2114

